PROTEINS: Structure, Function, and Bioinformatics 63:1005–1017 (2006)

Terminal Ion Pairs Stabilize the Second β-Hairpin of the B1 Domain of Protein G

Beatrice M. P. Huyghues-Despointes,[1] Xiaotoa Qu,[2] Jerry Tsai,[2] and J. Martin Scholtz[1,2]*
[1]*Department of Medical Biochemistry and Genetics, Texas A&M University, College Station, Texas*
[2]*Department of Biochemistry and Biophysics, Texas A&M University, College Station, Texas*

ABSTRACT **The effects of terminal ion pairs on the stability of a β-hairpin peptide corresponding to the C-terminal residues of the B1 domain of protein G were determined using thermal unfolding as monitored by nuclear magnetic resonance and circular dichroism spectroscopy. Molecular dynamics (MD) simulations were also performed to examine the effect of ion pairs on the structures. Eight peptides were studied including the wild type (G41) and the N-terminal modified sequences that had the first residue deleted (E42), replaced with a Lys (K41), or extended by an additional Gly (G40). Acetylated variants were made to examine the effect of removing the positive N-terminal charge on β-hairpin stability. The rank in stability determined experimentally is K41 > E42 ≈ G41 ≈ G40 > Ac-K41 > Ac-E42 ≈ Ac-G41 > Ac-G40. The T_m of the K41 peptide is 12 °C higher than G41, while the T_m values for the acetylated peptides are less than their unacetylated forms by more than 15 °C. NOE cross-peaks between side-chain methylene groups at the N- and C-termini and larger CαH shifts compared to random values are seen for K41. The addition of 20% methanol increases the stability in K41 and G41. The MD studies complement these results by showing that the charged N-terminus is important to stability. The type of ion pair observed varies with peptide, and when formed the simulations show that the ion pair can prevent fraying of the β-strands through electrostatic and hydrophobic contacts. Therefore, introducing favorable electrostatic interactions at the N- and C-termini can substantially enhance β-hairpin stability and help define the structure. Proteins 2006;63:1005–1017.**

Key words: β-turn; ion pair; main-chain hydrogen bond; hydrophobic contacts; NMR; circular dichroism; molecular dynamic simulations

INTRODUCTION

An elucidation of the physical properties that stabilize secondary structures, like α-helices, β-sheets, and β-hairpins, can lead to de novo protein design methods and should help to decipher the mechanism of the early steps in protein folding and misfolding. Unlike the studies on α-helices, a major problem has been finding appropriate β-hairpin and β-sheet model systems. The models employed are usually only marginally stable and/or tend to form undesirable aggregates in aqueous solution;[1] nevertheless, these features are often the properties that dictate proteins to particular folding pathways.[2]

The design of model systems is nonetheless valuable for understanding factors that determine β-sheet stability without potential complications of tertiary contacts with the rest of a protein. The results from model peptide and protein studies have revealed several factors that contribute to β-hairpin stability, including the amino acid intrinsic secondary structure propensities of the β-turn[3] and β-sheet,[4,5] short and long-range side-chain interactions, such as electrostatic and hydrophobic interactions, and main-chain hydrogen-bonding patterns.[1] Recently, short peptides (9–20 residues) that adopt monomeric β-hairpin[1] and β-sheet structures[6] in aqueous solution have been designed. These studies show that optimizing the turn sequence,[7,8] hydrophobic contacts,[9–11] and electrostatic interactions[8,12,13] in the peptide can stabilize β-hairpin formation. Furthermore, theoretical studies on β-hairpins have been used to model the early events of protein folding[14] and to elucidate the role that the β-turns, main-chain hydrogen bonding, and hydrophobic contacts have on folding and stability.[15–18]

The reference model for β-hairpin structure in many of these studies has been the peptide consisting of the C-terminal β-hairpin (residues 41–56) of the B1 domain of streptococcal IgG-binding protein G (G-hairpin). This was the first peptide shown to adopt a native-like β-hairpin structure in aqueous solution.[19,20] G-hairpin displays typical features that are considered good for β-sheet formation. Large contributions to stability of the β-hairpin are attributed to a well-defined β-turn and the hydrophobic cluster between the side chain of Val54 and the rings of

The Supplementary Material referred to in this article can be found online at http://www.interscience.wiley.com/jpages/0887-3585/suppmat/

Grant sponsor: National Institutes of Health; Grant number: GM-52483; Grant sponsor: Robert A. Welch Foundation; Grant numbers: BE-1281, A-1549.

*Correspondence to: J. Martin Scholtz, Department of Medical Biochemistry and Genetics, Texas A&M University, College Station, TX 77843-1114. E-mail: jm-scholtz@tamu.edu

Received 13 September 2005; Revised 16 November 2005; Accepted 5 December 2005

Published online 8 February 2006 in Wiley InterScience (www.interscience.wiley.com). DOI: 10.1002/prot.20916

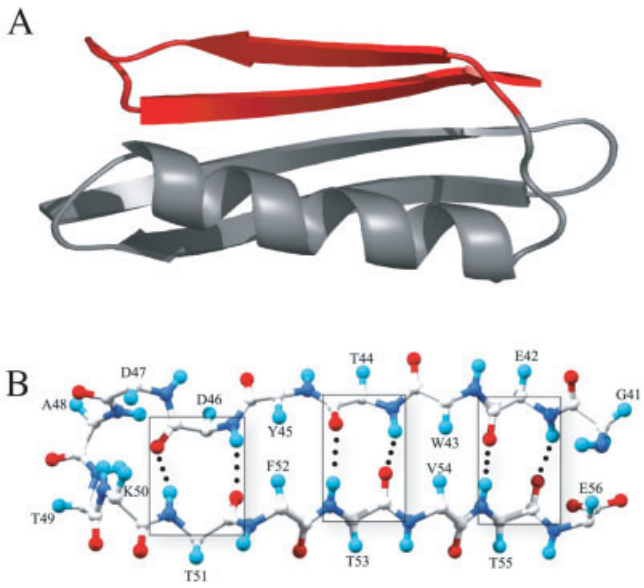

Fig. 1. **A:** A ribbon diagram (MOLSCRIPT[56]) of PGB1 (coordinates PDB: 1pgb[23]). The G-hairpin, residues 41 to 56, is highlighted in red. **B:** A ball-and-stick model of the backbone structure of G41. The hydrogen bonding patterns of the backbone at $\beta_{A,NHB}$ sites, defined in text, are shown in the boxed regions. The $\beta_{A,NHB}$ sites lie between the boxed regions. CαH, but not the side chains, are shown for clarity with the hydrophobic residues above the plane of the β-sheet and the hydrophilic residues below. The main-chain hydrogen bonds between the β-strands are shown. A hydrogen bond between the amino of Lys50, a β-turn residue, and the carbonyl of Asp46 is present in the crystal structure but not represented here.

three aromatic residues (Trp43, Tyr45, and Phe52) centrally located on one face of the β-hairpin.[20] Additionally, Thr, a good β-sheet forming residue,[4] is found throughout the sheet region.

The backbone structure of G-hairpin is shown in Figure 1. G-hairpin has six main-chain hydrogen bonds between the strands and one hydrogen bond between a β-turn residue Lys50 and a β-strand residue Asp46 (not represented in Fig. 1). According to the nomenclature proposed by Hutchinson et al.,[21] the $\beta_{A,HB}$ sites (the boxed sites) form two good inter-strand NH—CO backbone hydrogen bonds between the strands. The side chains at these sites usually favor aromatic and/or glycine residues in a survey of protein structures[21,22] and alternate in sequence with the $\beta_{A,NHB}$ sites where the backbone CO and NH groups point outward, excluding backbone hydrogen bonds. At the $\beta_{A,NHB}$ positions, pairs of β-branched or charge-charge residues are usually favored.[21,22] G-hairpin in the X-ray crystal structure of PGB1[23] consist of a β-hairpin with two $\beta_{A,NHB}$ sites, where hydrophobic residues interact on one face of the sheet and three $\beta_{A,HB}$ sites where either Thr/Asp, Glu, or Thr/Thr pairs lie on the opposite face. For G-hairpin and some stability-optimized variants,[8,10] the polar side chains are at $\beta_{A,HB}$ sites while the aromatic and hydrophobic side chains are at $\beta_{A,NHB}$ positions, in contrast to what is statistically observed. The hydrophobic cluster at the $\beta_{A,HB}$ site has also been observed in another model β-hairpin peptide, designed by Maynard et al.[24] from the β-strands of the DNA recognition motif of the *met* repressor protein dimer, suggesting that hydrophobic clusters at either site can be accommodated in the β-hairpin structure.

Based on a PROMOTIF analysis[25] of the crystal coordinates,[23] the β-turn, consisting of residues 47–50 (sequence DATK) of G-hairpin, is classified as a 4:4 type IV turn. The hydrogen bonds between carboxyl of Asp46 and the backbone NH of Ala48 and the side-chain hydroxyl of Thr49 prevent proper backbone hydrogen-bond angles and distances for the pairing of the CO of Asp47 and the NH of Lys50, precluding interactions necessary for a 2:2 type I β-turn.[26–28] At the termini, the end residues Gly41 and Glu56 are positioned at a non-hydrogen bonded site. Penel et al.[29] analyzed different types of β-strands in a group of non-homologous protein structures and observed that the end residues of a β-hairpin are more likely to end in a non-hydrogen bonded site because of closer side-chain packing at these sites. We suggest, additionally, that electrostatic interactions between the charged N- and C-termini, or between their side chains in the peptide at non-hydrogen-bonded ends, can possibly stabilize and reinforce the β-hairpin structure.

The thermodynamic stability of G-hairpin[30] and variants with single alanine substitutions[31] were determined by monitoring the temperature dependence of proton chemical shifts using one-dimensional nuclear magnetic resonance (NMR) spectroscopy. Honda et al.[30] showed importantly that there is a similar temperature dependence for all the nonpolar side chains and the α-proton signals of G-hairpin, suggesting that residues have the same cooperative two-state folding transition between the β-hairpin and unfolded states. The cooperativity of unfolding was confirmed by calorimetric experiments. Maynard et al.[24] have shown also that the thermal unfolding of another model β-hairpin 16-residue peptide can be analyzed assuming a cooperative two-state process by similar analysis. In a more recent study,[8] other variants of the 16-residue G-hairpin exhibit cooperative thermal transitions by coincident changes in the chemical shifts of the CαH, NH, and side chain CH_3 protons; however, residues in shorter peptide models do not all follow the same cooperative folding transition.[32] These results provide evidence that reasonable estimates of the β-hairpin stability for G-hairpin and peptide variants of similar lengths (16 or more residues) can be obtained by this NMR method.

Our goal here is to develop experimental and theoretical methods to further understand interactions that stabilize β-hairpin peptides in water. This study was inspired by the molecular dynamics results of Tsai and Levitt[33] that suggest wild-type G-hairpin can be stabilized by N- and C-terminal ion-pair interactions. Relatively few other studies on the role of interactions between the termini have been performed because of the belief that fraying of the termini diminishes the role that the terminal residues contribute to β-hairpin stability. Here, we test the idea that modifications of the N-terminus to change the position and number of favorable electrostatic interactions at the ends of the β-hairpin can have an effect on the stability

of the β-hairpin. We use the NMR procedure utilized by Honda et al.[30] to measure the effect on the β-hairpin stability of N-terminal modifications in the G-hairpin. We identify structural differences by 2D NMR and corroborate these results with differences in spectral features by circular dichroism (CD) spectroscopy. We also analyze MD-generated ensembles of β-hairpin structures for each variant to model the effect of modifying electrostatic interactions at the termini on the conformation of the peptides.

MATERIALS AND METHODS

Peptide Synthesis and Purification

The first C-terminal fifteen residues of the peptides were synthesized on Wang Resin support in one batch at Biopeptide Co. (San Diego, CA) by an automated solid-phase method using an active ester coupling procedure with Fmoc-amino acids. The last amino acid on each peptide was manually attached to the core peptide on the resin by similar methods to produce peptides with altered N-terminal amino acids and/or acetylated ends. The peptides were cleaved from the resin and deprotected by using a mixture of 2% anisole, 3% ethanedithiol, 5% thioanisole, and 90% trifluoroacetic acid. The peptides were not very soluble at low pH and contain a Thr deletion contaminant that co-eluted with the peptides of interest. As a result, the peptides were purified and separated from the contaminant by reversed-phase HPLC using Water Prep LC with a Delta-Pak C18 column in 10 mM sodium phosphate/acetonitrile gradient at pH 7.0. The peptides were further purified using a Pharmacia FPLC and a Pep RPC column in ammonium bicarbonate. The primary-ion molecular weight of each peptide and purity was confirmed by MALDI mass spectrometry. The resulting samples were $>$ 95% pure. Peptide concentrations were determined by the Edelhoch method using a $\epsilon_{(280\ \mathrm{nm})} = 6970\ \mathrm{M}^{-1}\ \mathrm{cm}^{-1}$ in 6 M GdnHCl in 20 mM sodium phosphate at pH 6.5.[34]

NMR Spectroscopy

Samples for NMR measurements were prepared by dissolving approximately 1 mM lyophilized peptide in either 9:1 mixture of H_2O and D_2O or in 99.8% D_2O in 5 mM sodium phosphate buffer. The pH was adjusted to 7 with a small amount of concentrated DCl or NaOD. The pH value was not corrected for solvent isotope effects. The ^{1}H chemical shifts values were referenced internally using 2,2-dimethyl-2-silapentane-5-sulfonate (DSS). NMR spectra were acquired on 500- and 600-MHz Varian Inova spectrometers and processed using NMRPipe.[35] One-dimensional NMR spectra were obtained by accumulating 256 scans consisting of 4,096 complex points and a spectral width of 6,000 with increasing temperature from 3 ° to 70 °C for the aqueous samples and −15 ° to 70 °C for the methanol samples at approximately 5 °C intervals. The difference in chemical shift between the methyl and hydroxyl resonances of 100% methanol was used to calibrate the probe temperature.[36] TOCSY spectra, applied with 30-ms mixing time and NOESY spectra, using a 200-ms mixing time, were acquired in both D_2O and 9:1 mixture of H_2O and D_2O solutions.

Thermodynamic Analysis

The changes in chemical shift with temperature for the peptides were analyzed assuming a two-state folding transition between native β-hairpin and denatured forms. The Tyr45 CδH chemical shift resonances were chosen because they were well separated from other resonances in a 1D ^{1}H NMR experiment and showed one of the largest changes in chemical shift with temperature. The thermal unfolding curves were fit by

$$y = \frac{y_U + y_F e^{\frac{\Delta H_m}{R}(1/T - 1/T_m)}}{1 + e^{\frac{\Delta H_m}{R}(1/T - 1/T_m)}} \quad (1)$$

where y_U is the unfolded baseline, y_F is the native baseline, T_m is the midpoint of the thermal unfolding curve, and ΔH_m is the enthalpy change at the T_m.

Spectral Measurements

Circular dichroism (CD) measurements were made on AVIV 62DS or 202SF spectropolarimeters using a NesLab coolflow CFT-33 refrigerated recirculator. The ellipticity is reported as mean residue ellipticity, (deg cm^2 dmol^{-1}), and was calibrated with (+)-10-camphorsulfonic acid. CD spectra were taken between 195 and 260 nm. Each spectrum was an average of 3 scans measured every 0.2 nm with an averaging time of 3 s and was smoothed using the AVIV software. The β-hairpin structure in each peptide was determined by monitoring the ellipticity at 230 nm at varying temperatures, pH, and salt concentrations. Samples were prepared by either diluting the aqueous stock solutions in varying concentrations of NaCl and cosolvent buffered with 5 mM sodium phosphate at pH 7.0 or in 1 mM sodium citrate, 1 mM sodium, and 1 mM sodium borate (CD buffer) at different pH values.

Generating and Analyzing MD Ensembles

We performed a total of 108 simulations for 10 ns each using the ENCAD program and the F3C water model.[37,38] The coordinates of the G-hairpin were taken from the C-terminal residues 41 to 56 of 1PGB crystal structure,[23] placed in a box of water, and minimized. The box of water was trimmed so that the edges were at least 8 Å away from the closest protein atom. All waters within 1.67 Å of the protein were removed, and the box sides were corrected to match the density of water (0.997 g/ml) at 298 K.[39,40] The average box size was 28.08 ± 0.5 Å, 43.64 ± 0.12 Å, and 27.64 ± 0.9 Å. The number of water molecules for each variant ranged from 1,028 for Ac-K41 to 1,058 for G41. Sodium or chloride ions replaced water molecules at random positions to yield an electrically neutral system. Conjugate gradient energy minimization steps were performed in the following order: The protein was fixed while the water molecules were minimized over the first 1,000 steps. The protein was then minimized in the next 1,000 steps, holding the water molecules fixed. The whole system was then minimized in the last 1,000 steps. To start different simulations, the system was equilibrated to 298 K with different random-seed numbers. During the calcu-

lations, the coordinates of the structure were updated at two femtosecond intervals and sampled every picosecond (or 500 steps). Each 10-ns simulation generated 10,000 structures. The variants were generated for the simulations by modifying the residues at the N-terminus in the crystal structure of G-hairpin. The coordinates of backbone atoms remained unchanged in the modified structure while the side-chain atoms were either deleted or regenerated at the N-terminus with ENCAD using standard residue conformations before the waters were added.

Programs written in C and PERL were used to analyze the structures of the peptide ensembles and were viewed using PyMol.[41] Only structures between 1–10 nanoseconds were used to analyze the β-hairpin interactions (hydrogen bonds, hydrophobic contacts, and ion pairs). For each β-hairpin variant, properties were averaged over all ensembles. CαRMSD values (α-carbon root-mean-square deviations) were calculated using the method of Kabsch.[42] Then, CαRMSD frequencies were calculated and represented using the R package.[43] Hydrogen bonds were defined as those between the donor hydrogen and the acceptor oxygen using a distance between hydrogen and oxygen to be less than 2.6 Å and the angle formed by the acceptor oxygen, hydrogen, and the donor atom to be greater than 120°. The definition of an ion pair was based on a simple distance cutoff, which is 3.5 Å between the positively charged nitrogen of the amino group and the negatively charged oxygen of the carboxyl group. Because a salt-bridge interaction is a hydrogen-bonded ion pair, its definition required satisfying both the hydrogen bond and ion-pair definitions. The hydrophobic contact surface area or HCSA was calculated using the Voronoi polyhedra method.[44] Two carbon atoms sharing a polyhedron face are considered a contact and the area of that face is defined as HCSA of such contact. Finally, hydrophobic clusters were defined by the largest side-chain to side-chain contact network. For example, if residue 41 contacts residue 42 and residue 42 contacts residue 43, then all residues were considered to belong to one cluster.

TABLE I. β-Hairpin Peptide Sequences

Name	Sequence[a] $\subset_{C}^{N}$	Terminal ion pairs[b]
G41 (WT)	A-D-D-Y-T-W-E-G | T-K-T-F-T-V-T-E	2
Ac-G41	A-D-D-Y-T-W-E-G-**Ac** | T-K-T-F-T-V-T-E	0
K41	A-D-D-Y-T-W-E-**K** | T-K-T-F-T-V-T-E	4
Ac-K41	A-D-D-Y-T-W-E-**K-Ac** | T-K-T-F-T-V-T-E	2
G40	A-D-D-Y-T-W-E-G-**G** | T-K-T-F-T-V-T-E	2
Ac-G40	A-D-D-Y-T-W-E-G-**G-Ac** | T-K-T-F-T-V-T-E	0
E42	A-D-D-Y-T-W-**E** | T-K-T-F-T-V-T-E	2
Ac-E42	A-D-D-Y-T-W-**E-Ac** | T-K-T-F-T-V-T-E	0

[a]Modifications are in bold.
[b]Total potential ion pairs that can form between the terminal residues of the β-hairpin.

RESULTS AND DISCUSSION

A Monomeric and Soluble Model

The G-hairpin peptide and variants of this sequence have been shown previously[20,31] not to form appreciable aggregates at the concentration needed for spectroscopic and NMR measurements. In this study, we take advantage of this system to make four modifications at the N-terminus of G-hairpin, as shown in Table I, to alter the number of and the distance between the ion-pair interactions at the ends of the β-strands: (1) Gly41 is deleted in peptide E42 causing the N-terminal strand to be one residue shorter than the C-terminal strand. (2) An additional Gly residue in peptide G40 is added at the N-terminus making the N-terminal strand one residue longer than the C-terminal strand. (3) Gly41 is replaced with a Lys residue in K41 to increase the number from 2 to 4 potential favorable ion pairs at the β-hairpin ends. (4) The four different peptide sequences are also acetylated at their N-terminus to prevent possible ion-pair interactions between the N-terminus and the other charge groups. It is important to note, however, that in the acetylated variants the carbonyl of the acetylated N-terminus can make possible hydrogen-bond interactions to the main-chain amino groups at the C-terminus. We identify also in Table I the number of favorable ion-pair interactions that each peptide can make potentially between the N- and C-termini. K41 can make possibly four ion-pair interactions at the ends, while the other non-acetylated variants can make only two. Only Ac-K41 of the acetylated peptides can potentially form two ion-pair interactions.

Our results on the variants in Table I show that they do not aggregate appreciably below 1 mM concentrations. The NMR chemical shifts and line widths for K41 are independent of peptide concentrations in the range of 0.2 to 0.7 mM, which suggests the peptide remains monomeric at these concentrations (data not shown). At concentrations higher than 1 mM, line broadening of the chemical resonances for K41 was apparent. As a result, the NMR experiments for K41 were performed at peptide concentrations below 1 mM. The other peptides at concentrations of 1–1.5 mM showed no apparent change in NMR spectral properties that would suggest aggregation. Additionally, no dependence of peptide concentration with ellipticity was found in the CD experiments. The mean residue ellipticity of each spectrum was the same at two different peptide concentrations that varied 10-fold (40 and 400 μM) which is consistent with the NMR results.

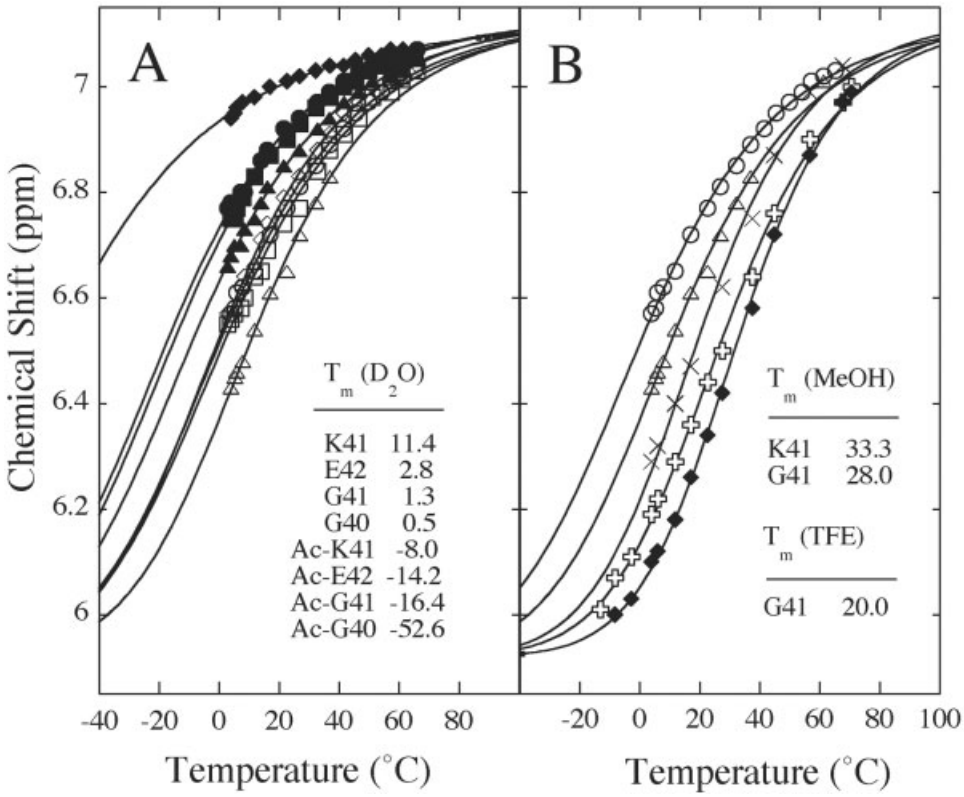

Fig. 2. Thermal unfolding monitored by the change in chemical shift of δH protons of Tyr45 with temperature. The T_m (°C) values for the peptides at specified conditions are also displayed. The curves are the fit to the data using equation 1. **A:** Curves for the β-hairpin variants [G41 (circles), E42 (squares), G40 (diamonds), and K41 (triangles)] in aqueous 5 mM sodium phosphate buffer. Open symbols represent variants with charged N-termini and closed symbols represent variants with acetylated N-termini. **B:** Thermal unfolding curves in 20% methanol (diamonds) for K41 and (crosses) for G41, and in 30 % TFE (X's) for G41, compared to corresponding curves in aqueous solutions (symbols are the same as in A).

Thermal Unfolding of β-Hairpin Structure by NMR

The folding rate of the G-hairpin (~10 μs at room temperature[45]) is fast relative to the NMR time scale; therefore, the NMR chemical shift signals of the peptide reflect an average value of the folded and unfolded fractions at equilibrium. Upon denaturation, the resonance signals move from the chemical shift of the native signal to those of the unfolded form. We measure the change in chemical shift with temperature of the Tyr45 CδH to access the stability of the G-hairpin variants. The results are shown in Figure 2 for all eight peptides. We observe that K41 has the greatest deviation from the unfolded chemical shift at low temperature, while Ac-G40 peptide has the smallest. Peptides with one residue extension or deletion at the N-terminus (G40 or E42) have very similar changes in the folded population with temperature as G41. N-terminal acetylation of all the peptides destabilize β-hairpin formation: Ac-K41, Ac-G41, and Ac-E42 are destabilized similarly compared to their uncapped forms, while Ac-G40 is substantially less stable than G40. The perturbations in chemical shift at 4 °C relative to the unfolded value at high temperature, a measure of the stability of the β-hairpin, are ranked in the following order: K41 > E42 ≈ G40 ≈ G41 > Ac-K41 > Ac-G41 ≈ Ac-E42 > Ac-G40. This rank is observed throughout the unfolding transition.

Since fully folded and unfolded chemical shift data for the G-hairpin are not attainable directly, it is difficult to determine how folded the peptides are at 4 °C in aqueous solution. Several methods to estimate the folded chemical shift baseline have been used previously. The folded baselines of G-hairpin have been estimated in 30% TFE,[20] when model hairpin peptides are cyclized,[46] by fitting the wild-type data,[31] or using a highly stabilized variant[8] directly. The chemical shifts of the unfolded baselines have been estimated by using the data from shorter random coil peptides with similar sequences by adjusting for temperature, solvent, and end charge effects ([8], and reference therein), unfolded variants at high temperatures,[31] or G-hairpin in 6 M urea.[47] These methods have estimated G-hairpin at 4 °C in aqueous solution to be in the range of 30–45% folded. In this study, we decided to estimate the folded baseline by measuring the thermal unfolding transition by NMR of K41 and G41 in methanol and TFE, cosolvents known to stabilize secondary structure in peptides (reviewed in [48]), where the occupation of native β-hairpin structure is larger than it is in aqueous solutions. We include here methanol as a cosolvent because we observe stabilization of the K41 β-hairpin by CD in methanol (see below) and methanol was shown also to stabilize other model β-hairpin peptides.[13,24] The results

TABLE II. A Summary of NOE Cross-Peaks in K41 Peptide[†]

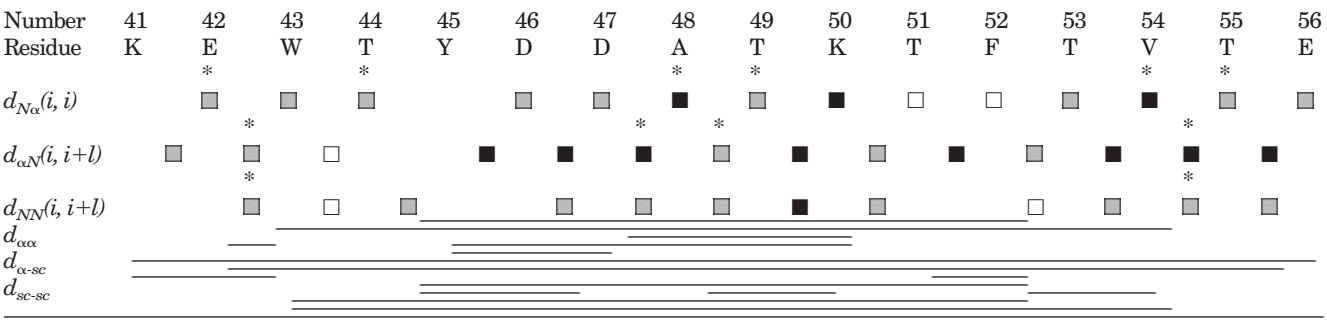

[†]The NOE intensities are proportional to the shading of the squares (white, weak; grey, medium; black, strong). Asterisks (*) indicate positions where sequential connectivities could not be established due to peak overlap. Lines represent connectivities between two residues. Data were obtained from peptide solutions in 10 and 100% D_2O in 5 mM sodium phosphate at pH 7.

for peptides G41 and K41 in 20% methanol and 30% TFE in comparison to the results in aqueous solution are shown in Figure 2(B). We were able to make measurements at temperatures below 0 °C (~ −15 °C) due to the depression of the freezing point of water in the cosolvents. The results in 20% methanol show that the chemical shifts of Tyr45 CδH in G41 and K41 begin to plateau at low temperatures below 0 °C and that the peptides seem be close to 100% folded at these temperatures. We fit all the curves in Figure 2(A,B) by equation 1 (See Materials and Methods) with a constant native and unfolded proton chemical shift values. We determine the folded baseline by using the 20% methanol curves for G41 and K41 (5.92 ppm) and the unfolded baseline value with the chemical shift value of the least stable variant, Ac-G40, at high temperature (7.14 ppm). The latter value is very similar to the random coil value for Tyr CδH.[49] We show the apparent T_m values for the variants in water and in cosolvents in Figure 2. We do not further quantitate the data because of the broad transition and the lack of good baselines for all the peptides. These results indicate that K41 and G41 are ~50% and ~30% folded, respectively, in aqueous solution at 4 °C, which is consistent with values for G41 determined previously.

Several interesting observations are apparent in the thermal unfolding of G41 and K41 in cosolvents: (1) Cosolvents tend to decrease the chemical shift values to more folded values. Samples in 20% methanol perturb the chemical shifts more than those in 30% TFE relative to the unfolded values, suggesting that β-hairpin is more stable in methanol than in TFE. (2) The proton chemical shifts in 20% methanol for G41 and K41 approach the same value at low temperature, suggesting that each cosolvent does induce full structure formation in the peptides. (3) The unfolded chemical shift values are similar to those in aqueous solution at high temperature, showing that these cosolvents do not alter the intrinsic random-coil proton chemical shift values.

Characteristics of β-Hairpin Structure by 2D ^{1}H-NMR

The proton chemical shift changes with temperature cannot identify if the N-terminal variants have β-hairpin structure. We turned instead to 2D ^{1}H-NMR techniques to identify if the G-hairpin variants fold like G41. Several characteristics identify β-hairpin structure, in general:

(1) The turn region has strong d_{NN} (i, i +1) and weak $d_{\alpha N}$ (i, i +1) NOEs (similar features are observed for α-helical conformation).
(2) The sheet region has weak d_{NN} (i, i +1) and strong $d_{\alpha N}$ (i, i +1) NOEs.
(3) Long-range NOE interactions ($d_{\alpha\alpha}$, $d_{\alpha sc(\text{side chain})}$, and d_{scsc}) are observed between residues in the turn and strands of the sheet.
(4) The differences in CαH chemical shift compared to the random coil values are negative for turn-like structures and positive for β-sheet structures.

The chemical shift assignments and the NOE cross-peaks for the peptides in aqueous solutions at 4 °C are consistent with those observed in G41, suggesting that the peptide variants are forming some degree of β-hairpin structure in solution. Differences in proton chemical shifts in the variants are small and are most noticeable for the N-terminal mutated residues (for example, the chemical shift of CαH of Glu42 changes by 0.4 ppm in E42). The summary of NOE patterns found for the most stable variant, K41, in water and D_2O are shown in Table II. The turn residues have strong d_{NN} (i, i +1) and weak $d_{\alpha N}$ (i, i +1) NOE cross-peaks while the β-sheet residues have weak d_{NN} (i, i +1) and strong $d_{\alpha N}$ (i, i +1) NOE cross-peaks consistent with β-hairpin structure. Similar NOE patterns observed for G41 are seen for K41. We note that new NOE side-chain interactions are detected in K41 between the side chains of Lys41 and Glu56 and of Glu42 and Thr55 and between the aromatic residues and Val54. These new NOE cross-peaks suggest that the ion pairs at the ends increase the hydrophobic contacts and help tether the N- and C-termini. Fewer NOE interactions are observed, however, in the less stable variants.

The chemical shifts of the CαH resonances of G41 and K41 in aqueous solution and 20% methanol are shown in Figure 3 and compared to the chemical shifts of the CαH resonances of the G41 sequence in B1 domain of protein G. The patterns observed in the protein are also observed for

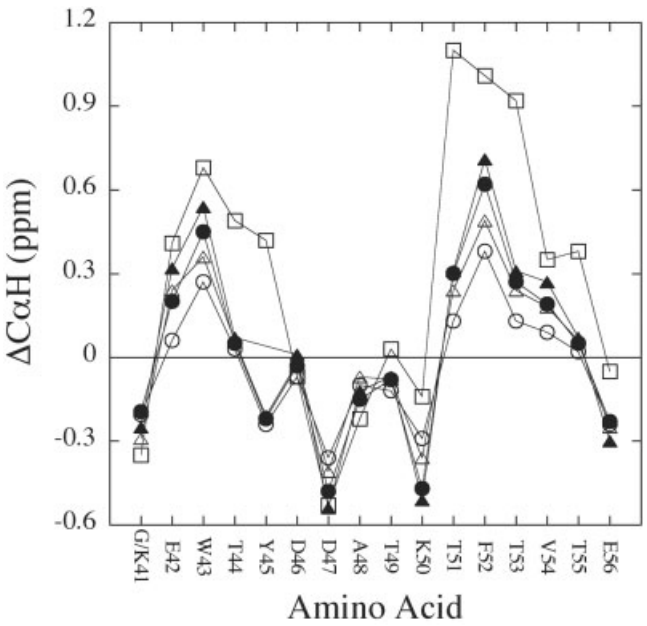

Fig. 3. CαH chemical shifts for each residue in the G41 (circles) and K41 (triangles) peptides and in the C-terminal region of PGB1(squares). Data in water and 20 % methanol are represented by open and closed symbols, respectively. CαH chemical shift deviations of the β-strand region are larger in the protein than that in the peptides while the β-turn CαH chemical shift deviations are similar.

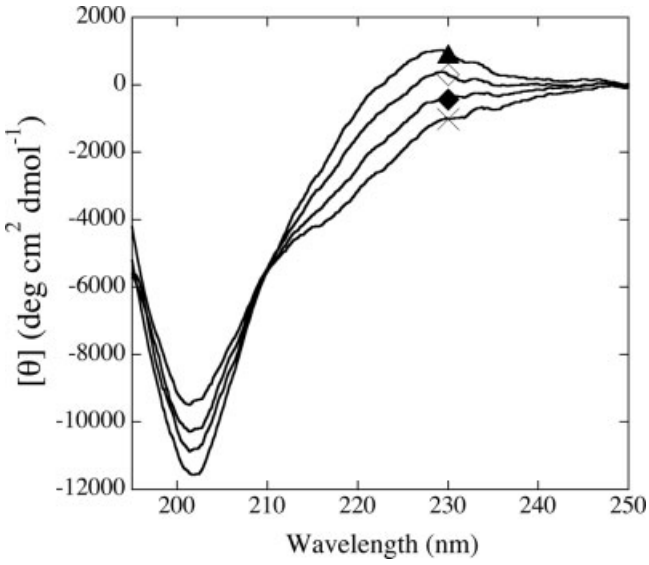

Fig. 4. CD spectra of the K41 peptide at 0 °C (triangles), 20 °C (open diamonds), 40 °C (closed diamonds), and 60 °C (X's). Solutions consisted of 100 μM peptide in 5 mM sodium phosphate at pH 7. Measurements were performed with a 1 mm cuvette.

the peptides in water and methanol, but the intensities are smaller in the latter. For residues in the sheet region (Glu42 to Tyr45 and Thr51 to Val54), positive changes in CαH chemical shifts are seen, while residues in the turn region show negative deviations. We observe that K41 has larger CαH chemical shift differences than G41, and the differences are larger in 20% methanol than in water, suggesting that K41 is more stable than G41 under all conditions.

Characteristics of β-Hairpin Conformation by Circular Dichroism

In addition to studying these peptides by NMR, we have examined the effect of pH, temperature, and cosolvent on the CD spectra of the eight peptides. The spectra show characteristics of midsize peptides (10–20 residues) that have a predominance of extended conformation.[50] The CD spectra of the 16-residue K41 peptide are shown at various temperatures in Figure 4. The spectra are similar to those observed for other variants at various temperatures (data not shown) and to the spectrum of G41 at 5 °C at pH 6.3 shown previously.[20] Two distinct bands, a small positive band at 230 nm and a negative band above 200 nm, are observed in the folded conformation at 0 °C. The spectra do not show a distinct negative band at 215 nm characteristic of a β-sheet conformation likely because of its short length, the contributions from the type IV turn involving 4 of its 16 residues, and the aromatic component to the CD signal of the Trp43.[51] We note that the 16-residue model peptide studied by Ciani et al.,[13] which lacks Trp residues and has a type I′ Asn-Gly two-residue turn sequence, does show a negative CD band at 215 nm at 25 °C, which becomes more negative in the presence of methanol.

The CD signals at 230 nm for the peptides (data not shown) rank in the same order as the stability measurements using the NMR chemical shift method. The positive band at 230 nm diminishes with decrease in stability of the peptides. The differences in CD signal between each peptide are, however, only slightly above the noise level of the experiment, precluding quantitative stability difference measurements by this method.

Both bands in the spectra of K41 at 0 °C in Figure 4 diminish in intensity with increasing temperature. An isodichroic point is observed near 210 nm when spectra at different temperatures are compared, suggesting that each residue in the peptide exists in one of two distinct conformations. Similar changes in the CD band at 230 nm with temperature in aqueous solutions were observed by Cochran et al.,[10] who replaced all hydrophobic residues with Trp residues in G-hairpin and Fesinmeyer et al.,[8] who enhanced hairpin stability in variants of G-hairpin by optimizing the turn and electrostatic interactions at the termini. Due to the contribution of multiple Trp chromophores to the CD signal, the positive band at 230 nm in these studies is substantially larger.

We studied the effects of pH, salt, and cosolvents on the CD spectra for G41 and K41. The dependence of the intensity of the band at 230 nm on pH is shown in Figure 5. K41 has a more positive band at 230 nm than G41 at all pH values, while the changes in $[\Theta]_{230\ nm}$ with pH for both peptides are similar. The signal at 230 nm increases (~500 deg cm^2 dmol^{-1}) as the pH is dropped below 5 and decreases above pH ~ 7.2. The change in $[\Theta]_{230\ nm}$ at high pH results from the titration of the N-terminus and shows that the charged N-terminus is stabilizing to β-hairpin structure at neutral pH. The low pH increase in $[\Theta]_{230\ nm}$

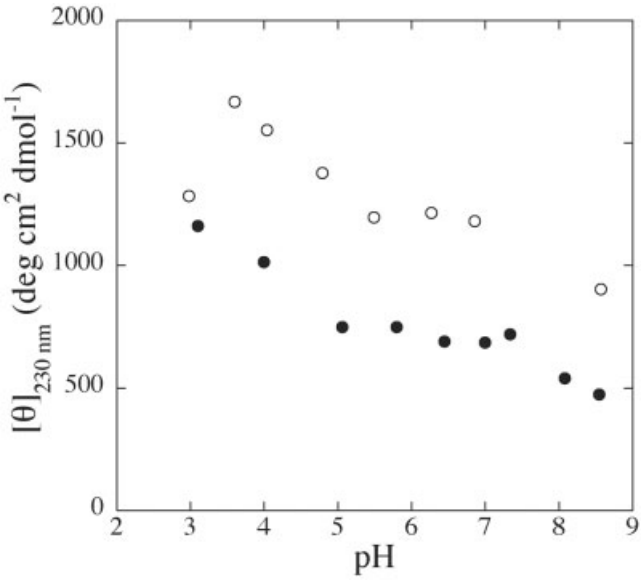

Fig. 5. The dependence of the CD signal at 230 nm on pH for G41 (closed circles) and K41 (open circles). Solutions consisted of 40 μM peptide in CD buffer and measurements were made with a 1 cm cuvette.

is caused by the protonation of carboxylate groups. At pH 7, the net charges are −3 and −2 for G41 and K41, respectively; as a result, the change in mean residue ellipticity at low pH suggests that repulsion between like-charged groups outweigh the contributions to stability of the favorable ion-pair interactions at the peptide ends. These results are supported by the effects of NaCl, a neutral Hofmiester salt, and Na_2SO_4, a stabilizing Hofmiester salt,[52] on the CD signal at pH 7. We observe only small increases in $[\Theta]_{230\ nm}$ (<500 deg cm^2 dmol^{-1}) with increasing salt concentrations for both G41 and K41 (data not shown) and observe similar results by NMR by monitoring chemical shift deviations. The T_m values for G41 or K41 in the presence of 0.4 M Na_2SO_4 were not substantially larger than in the absence of salt (increase in T_m of ~5 ° to 7 °C). The results from the pH and salt studies suggest that the stability at pH 7 is a result of a balance between favorable and unfavorable electrostatic interactions in these peptides.

The CD spectra of G41 and K41 in methanol were measured, and the results for the K41 peptide in methanol are shown in Figure 6. Similar results were observed for G41 (data not shown). The intensity of the positive band at 230 nm becomes more elevated with increasing amounts of methanol. The overall spectral characteristics in methanol are similar to the spectra in its absence, but the band shifts to slightly higher wavelengths in more methanol. An isodichroic point at 210 nm in 20% methanol is also observed with increasing temperature as shown in Figure 6. These results complement the NMR results that show larger chemical shifts deviations of Tyr45 CδH from the random values for G41 and K41 in 20% methanol than in its absence (Fig. 2).

Modeling Effects of Terminal Ion Pairing on β-Hairpin Geometry

The ensembles generated by the MD simulations of the eight variants of G-hairpin were analyzed to determine the effects of varying the electrostatic interactions at the termini on the conformation of the β-turn and β-strands. An efficient potential energy calculation was used, and long trajectories (10 ns) that give adequate sampling were performed. Since each MD trajectory follows only the progression over time of one molecule, several different simulations for each peptide (between 10–20 trajectories) were generated to provide a sampling of the average properties of the β-hairpin conformation. The number of simulations performed for each peptide is shown in Table III. We analyzed the structures by two methods: (1) The MD structures were compared to residues 41–56 excised from the crystal structure of 1pgb using the CαRMSD. This method assumes that the most stable conformations of the peptides in solution should be identical to the conformation in the protein. Nevertheless, this comparison provides the most effective method to display the possibility of large deviations from β-hairpin structure. (2) The populations of the β-hairpin-like characteristics (main-chain H-bond, hydrophobic and ion-pair interactions between the side chains, and the β-turn and β-strand torsion angles) were analyzed and compared in the generated structures. The benefit of this method is that the simulated structures can be compared to each other rather than to a reference model β-hairpin structure and distribution of average properties of the structures can be determined.

Table III shows also how often and what type of terminal ion-pair interaction forms in the ensemble of structures. Ac-G41, Ac-G40, and Ac-E42 cannot form terminal ion pairs because there is no charged amino group at the N-terminus. K41 and G40 form ion pairs more than 90% of the time, and since K41 can form potentially two simultaneous ion-pair contacts (4 potential ion pairs), we observe that more than one type is populated (occupancy of 1.1 for K41). G41 and E42 can make only one of two potential ion pairs, which exist in about 60% of the structures. Additionally, salt-bridge interactions (defined as hydrogen-bonded ion pairs) can be determined by measuring the proper hydrogen-bond geometry (see Materials and Methods). Most of the ion pairs formed in the simulations are salt bridges as shown in Table III. Interestingly, each variant favors different combinations of terminal ion-pair groups. When G41 formed ion pairs, the terminal amino group interacted with either the side chain or the C-terminal carboxyl group; all other variants preferred mainly one type of ion pair.

The importance of ion pairs in sustaining low CαRMSD values during the simulations is shown in Figure 7 where three individual trajectories of G41 are shown in Figure 7(A), and the distance between the charged groups on the terminal residues, Gly41 and Glu56, over the three trajectories are shown in Figure 7(B). When ion pairs are formed, a lower CαRMSD is seen throughout the trajectory, whereas when ion pairs are not formed, the structures have CαRMSD that increase over the entire trajec-

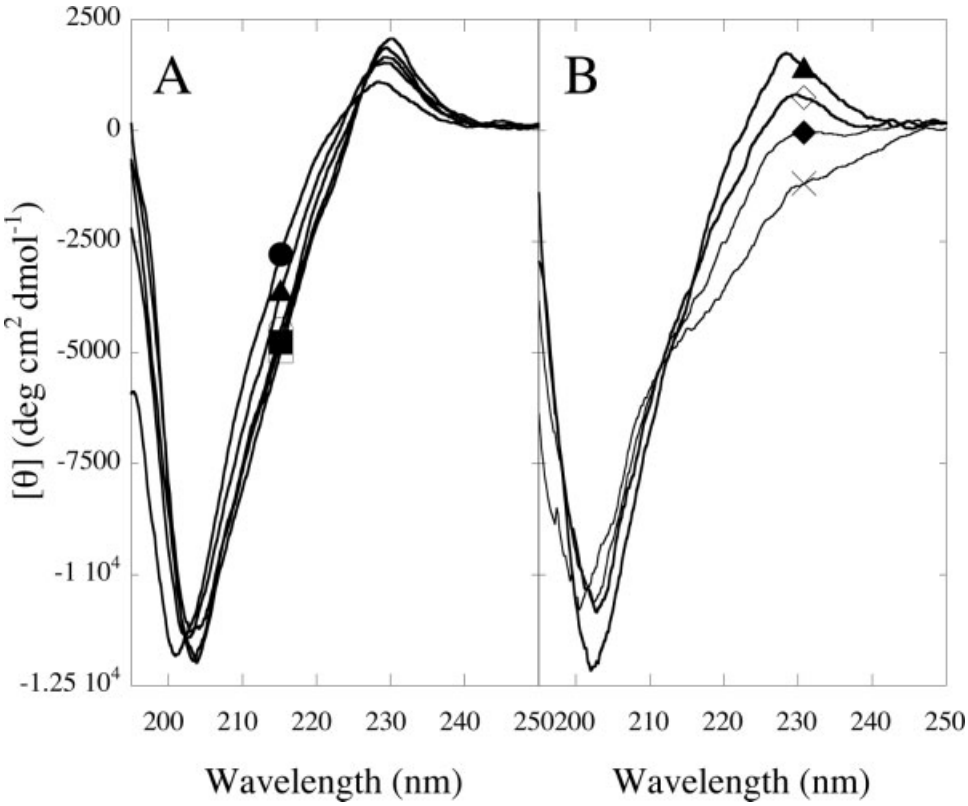

Fig. 6. **A:** CD spectra of K41 peptide in various methanol concentrations [0% (closed circles), 20% (closed triangles), 30% (open circles), 40% (closed squares), and 50% (open squares)]. **B:** CD spectra of K41 in 20 % methanol at 0 °C (closed triangles), 25 °C (open diamonds), 45 °C (closed diamonds), and 75 °C (X's). Solutions consisted of 100 μM peptide in 5 mM sodium phosphate at pH 7. Measurements were made with a 1-mm cuvette.

TABLE III. Terminal Ion-Pair (IP) Interactions in the Ensembles of MD-Generated Structures

Property	Category	G41	K41	E42	G40	Ac-G41	Ac-K41	Ac-E42	Ac-G40
Trajectories[a]		20	20	10	18	10	10	10	10
Terminal IP	*Possible IP*[b]	2	4	2	2	0	2	0	0
	IP[c]	0.6	1.1	0.6	1.0	—	0.9	—	—
	SB (%)[d]	92	78	84	70	—	65	—	—
Type of terminal IP[e]	*Nm to Os*	0.2	0.0	0.0	0.9	—	—	—	—
	Nm to Om	0.4	0.1	0.6	0.1	—	—	—	—
	Ns to Os	—	0.0	—	—	—	0.1	—	—
	Ns to Om	—	1.0	—	—	—	0.8	—	—
	Schematic[f]								

[a]Number of simulations performed for each peptide.
[b]The total number of potential ion pairs (IP) involving the N- and C-terminal residues.
[c]The average number of ion pairs in the ensemble of structures. The dashes indicate no ion pair.
[d]The percent occurrence that the ion pairs also form salt bridges, defined by distance and angle restraints for hydrogen bonds.
[e]The type of potential terminal ion pairs include N-terminal (Nm) or Lys41 side chain amino group (Ns) to C-terminal (Om) or Glu56 side-chain carboxyl (Os). Dashes indicate not significantly populated.
[f]Representation of possible terminal ion pairs between the backbone and side chains with amino groups in black, carboxyls groups in grey, and the acetyls groups in white.

tory. In particular, the appearance of an ion pair midway through a simulation seems to stabilize the structure from further deviations. We observe the same trend for other peptides; when structures form ion pairs at the termini, the average CαRMSD and standard deviations are lower than for structures without ion pairs.

The CαRMSD values of all measured ensembles for each variant were normalized to determine the distribution of

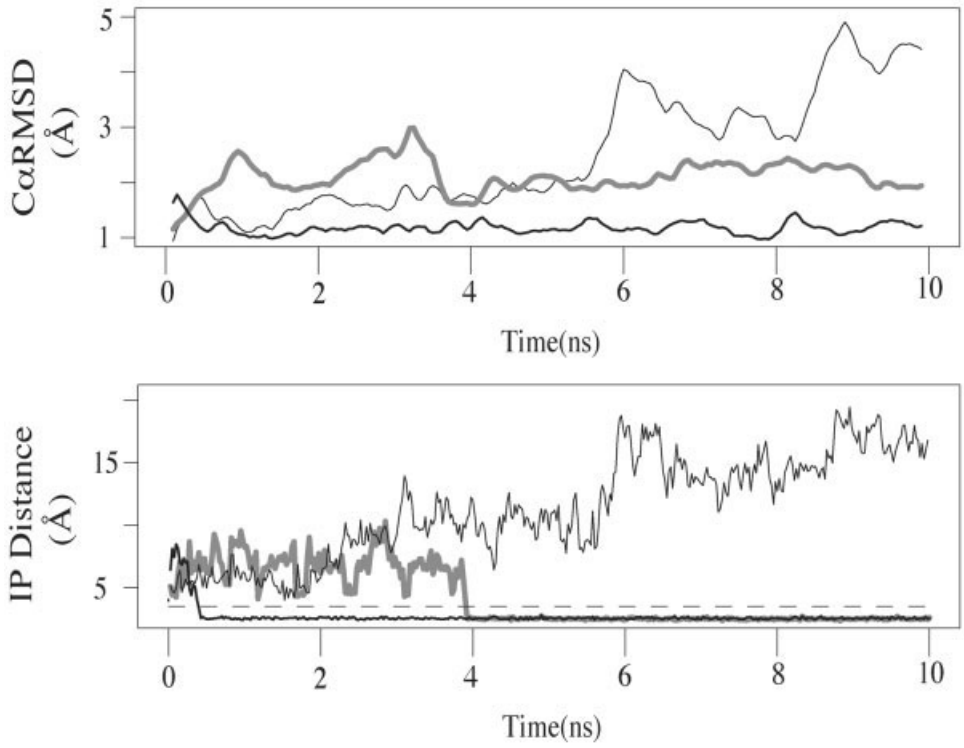

Fig. 7. Three CαRMSD curves of three individual trajectories of G41 over 10 ns (**A**) were compared to the ion pair (IP) distance between the charged N- and C- termini (**B**). One trajectory has no ion pairs formed (thin dark line); another trajectory has the ion pair formed halfway through the simulation (thick gray line); the last trajectory has the ion pair formed completely throughout the simulation (thick dark line). The dashed line at 3.5 Å in B is the distance cut-off for ion-pair formation. Any structures below that line are counted as having ion pairs.

CαRMSD values as shown by the population distributions in CαRMSD in Figure 8. Although the same CαRMSD value does not imply the same structure, the shape of the CαRMSD distribution suggests ensembles share similar features with a single, narrow distribution indicating structures with less variation. The differences between non-acetylated and acetylated β-hairpin variants are clear: the populations of non-acetylated β-hairpins generally show narrow CαRMSD distributions with mean values below 2.5 Å, while the acetylated β-hairpin distributions show higher mean values and larger distributions ranging from below 2 Å to above 4 Å. The CαRMSD data do not show, however, clear demarcations in population differences for the non-acetylated or acetylated peptides that were observed experimentally by their thermal stabilities. The largest CαRMSD values were observed in the strand region while less than 0.3 Å deviations were observed in the β-turn region. For all variants, the β-turn remained quite stable throughout the simulations and similar to the Type IV β-hairpin of G-hairpin in the protein crystal structure. It is also important to note that the CαRMSD for all simulated structures were at least 1.2 Å different from the starting structure indicating that the conformation is different between the G-hairpin in solution and when packed in the protein crystal structure.

A detailed analysis of the average backbone torsion angles, main-chain hydrogen bonds, and hydrophobic contact surface area (HCSA) displayed by the ensemble of structures in each variant are shown in the Supplementary Table IV. A summary of the general features of the analysis is described below.

The β-strand conformation can be defined by backbone torsion angles of $\phi = -180$ to $-30°$ and $\psi = +60$ to $+180°$ and -180 to $-150°$.[53,54] Our results show that the average β-sheet conformation ranges from 50 to 58% for the variant structures. As expected, residues near the β-turn (Asp46 and Thr51) adopt the β-sheet conformation more often than residues near the termini. Additionally, we note that residues on the hydrophobic side (Trp43, Tyr45, Phe52, and Val54) exist more often, on average, in β-sheet conformations than the residues on the hydrophilic side (Glu42, Thr44, Thr53, and Thr55). As shown in Figure 1, the $\beta_{A,NHB}$ residues point toward each other forming a hydrophobic cluster. To retain this cluster, they must favor β-sheet conformations at these positions. The $\beta_{A,HB}$ residues face away from each other and interact with solvent and do not retain β-sheet conformations as often.

There are seven native main-chain hydrogen bonds observed in G-hairpin in the PGB1 crystal structure [Fig. 1(B)]. The results show that native hydrogen bonds form more often near the β-turn than the termini. Non-native hydrogen-bonds exist also between the main-chain β-strands in the ensemble, but their frequencies are low. K41 makes on average fewer native and non-native back-

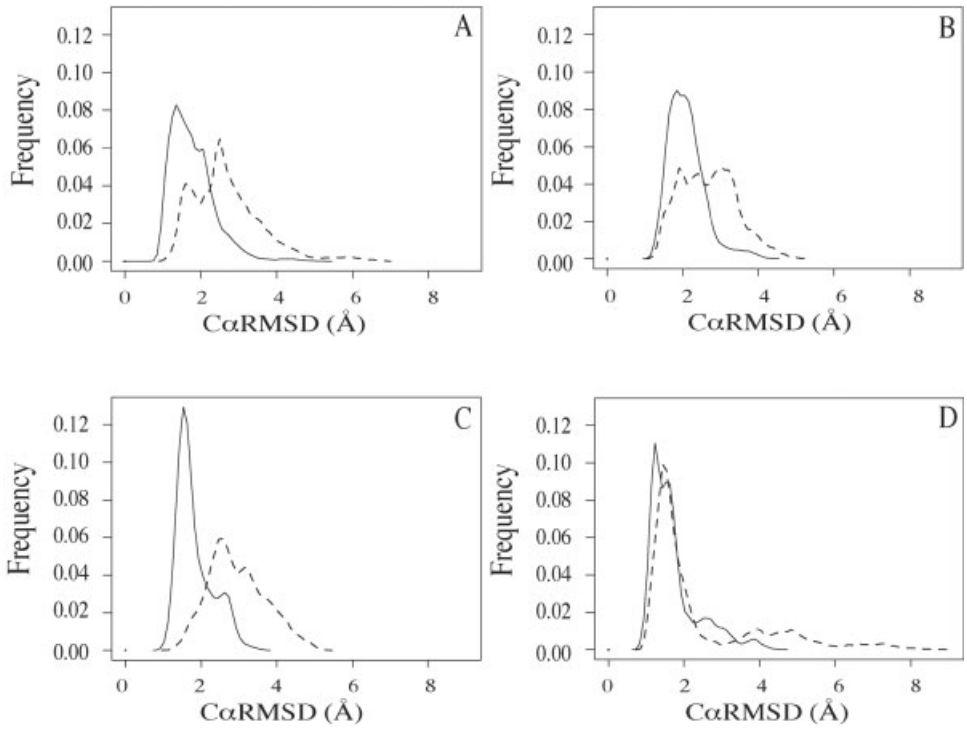

Fig. 8. Probability distributions of the normalized CαRMSD in the MD-generated ensemble of structures are shown for (**A**) G41/Ac-G41, (**B**) K41/Ac-K41, (**C**) G40/Ac-G40, (**D**) E42/Ac-E42. The non-acetylated peptides are shown with solid lines, while the acetylated peptides are shown with dashed lines.

bone hydrogen bonds than the other peptides do, suggesting that the terminal ion-pair interaction prevents proper backbone hydrogen-bond formation in K41. We also observe that the carbonyl groups of the acetyl of Ac-E42, Ac-G41, and Ac-K41 can hydrogen bond to main-chain amino groups of either Thr55 and Glu56 in >50% of the ensemble structures. In contrast, an extra Gly at the N-terminus of Ac-G40 (see Table I) places the main chain hydrogen-bonding groups and the acetyl carbonyl too far from the C-terminus to make significant hydrogen bonds to the opposite strands (<5% of the ensemble structures, data not shown). These results can explain why Ac-G40 is more destabilized experimentally than the other acetylated variants. In addition, we analyze the hydrogen-bond patterns of main-chain groups with the surrounding solvent water (data not shown). Only the terminal main-chain groups interact with water significantly, and of all the variants, Ac-G40 shows the strongest tendency to interact with water, suggesting a relatively open, less stable structure. The populations of backbone torsion angles and native hydrogen bonds provide evidence that the β-strand ends fray.

The packing contributions are determined by calculating the average HCSA and by identifying residues that participate in the major "cluster" of buried surface area. The side-chain packing in the peptides buries from 79 to 95 $Å^2$ of HCSA in the strand region and more than 75% of the total HCSA for the peptides is made up of the largest hydrophobic cluster (see Materials and Methods), involving the four interior hydrophobic residues, Trp43, Tyr45, Phe52, and Val54. K41 and Ac-K41 produce the largest clustered HCSA, while Ac-E42 has the smallest.

Although the type of terminal ion pair can vary with the modifications at the N-terminus, our analysis shows that ion pairs form with all variants that have charged groups at their N-termini. The MD results show that terminal ion-pair interactions are significantly formed in the ensemble of structures and do not disrupt the β-turn conformation. Furthermore, in over 65% of the structures, ion pairs form hydrogen bonds making them salt-bridge interactions and signifying interactions with well-defined distance and geometric restraints. We show also that the structures vary less and have overall smaller CαRMSD when a peptide has a charged N-terminus rather than when the N-terminus is acetylated.

Salt bridges across the termini help stabilize the β-hairpin by preventing the strands from fraying. Since G-hairpin ends with non-hydrogen-bonded residues, the presence of a terminal ion pair interaction can act as a pseudo-hydrogen-bond ring.[21] For example, in the K41 simulations, the termini interact by the side chain of Lys41 and the main-chain carboxyl of Glu56 in almost all structures. The calculations with K41 supports the experimental results where NOE contacts are observed between the Cα proton of Glu56 and the methylene protons of Lys41, suggesting this ion pair is formed in solution. Furthermore, the MD simulations show that a terminal ion pair can affect main-chain hydrogen-bond patterns and increase hydrophobic contacts, as shown by the interactions of the side-chain methylene groups of K41 with major

hydrophobic cluster. Thus, the MD simulations of the G-hairpin variants provide a structural picture of the important molecular interactions that can stabilize the β-hairpin structure in solution.

CONCLUSIONS

Favorable Electrostatic Interactions at the Termini Stabilize β-Hairpin Formation

The data show that increasing the number of favorable ion-pair interactions provides increased β-hairpin stability while decreasing the number of interactions by N-terminal acetylation can destabilize the β-hairpin structure. K41 has the largest number of potential ion-pair groups in our data set and is more stable than the other peptides. Likewise, Ac-K41, which can potentially make two favorable ion-pair interactions at the termini, is more stable than the other acetylated peptides that cannot make similar interactions. We observe that K41 has increased thermal stability, an increased number and more intense NOE cross-peaks in the hydrophobic cluster and at the terminal side-chain residues. It also has larger CαH chemical shift deviations from random values than variants lacking the attractive interactions. Conversely, removing the charged N-terminus by acetylation has the opposite affect; all acetylated peptides are less stable to thermal denaturation than their N-terminal charged versions. It also worthy to note that moving the position of the charged N-terminus by one residue has minimal affect on β-hairpin stability. E42 and G40 have comparable stabilities to G41; similar electrostatic interactions are likely present in all three peptides. When the peptides are acetylated, however, the three peptides no longer have similar stabilities. G40, the longer peptide, is more destabilized and likely does not make the extra hydrogen bond between the acetyl group and the C-terminus that the other acetyl peptides are able to make.

The results show also that the stability can be enhanced in cosolvents, methanol and TFE, and by NMR chemical shift analysis nearly 100% β-hairpin population can be achieved in 20% methanol at −10 °C. Additionally, pH and salt studies suggest that the electrostatic interactions are not optimal for the stability of these peptides. We have further data suggesting that G-hairpin variants without these unfavorable interactions have greater stability than K41 at pH 7 (unpublished results).

In conclusion, we show here that introducing single modifications to the N-terminal residue can affect the stability without altering the overall conformation of G-hairpin. Recently, several groups have shown that β-hairpin stability can be increased by introducing multiple ion-pairs interactions throughout the sheet region,[13] at the sequence ends of non G-hairpin models,[12,55] or in a stabilized variant of G-hairpin (optimized for the turn and hydrophobic clustering).[8] We show here that just a simple replacement of the first residue or acetylation of the N-terminus can affect the stability of G-hairpin. These results, in combination with these previous studies, show convincingly that favorable electrostatic interactions can effectively increase the stability of β-hairpin structure in many different model peptide systems in solution. We show also that the wild-type G-hairpin (G41) is stabilized by ion pairs at the N- and C-termini as was suggested by the molecular dynamic simulations of Tsai and Levitt.[33] The MD data suggest here that optimizing favorable electrostatics interactions at the N- and C-termini can reinforce the hydrophobic interactions and confine the ends to enhance β-hairpin stability.

ACKNOWLEDGMENTS

We thank the Protein Chemistry and Biomolecular NMR laboratories at Texas A&M University for assistance, and Yun Wei for many helpful discussions and careful reading of the manuscript. This work was sponsored in part by grants BE-1281 (J.M.S.) and A-1549 (J.T.) from the Robert A. Welch Foundation.

REFERENCES

1. Ramírez-Alvarado M, Kortemme T, Blanco F, Serrano L. β-hairpin and β-sheet formation in designed linear peptides. Bioorg Med Chem 1999;7:93–103.
2. Baldwin RL, Rose GD. Is protein folding hierarchic? I. Local structure and peptide folding. Trends Biochem Sci 1999;24:26–33.
3. Hutchinson EG, Thornton JM. A revised set of potentials for beta turn formation in proteins. Protein Sci 1994;3:2207–2216.
4. Smith CK, Withka JM, Regan L. A thermodynamic scale for β-sheet forming tendencies of the amino acids. Biochemistry 1994;33:5510–5517.
5. Smith CK, Regan L. Guidelines for protein design: the energetics of beta sheet side-chain interactions. Science 1995;270:980–982.
6. Lacroix E, Kortemme T, Lopez de la Paz M, Serrano L. The design of linear peptides that fold as monomeric beta-sheet structures. Curr Opin Struct Biol 1999;9:487–493.
7. Espinosa JF, Syud FA, Gellman SH. Analysis of the factors that stabilize a designed two-stranded antiparallel β-sheet. Protein Sci 2002;11:1492–1505.
8. Fesinmeyer RM, Hudson FM, Andersen NH. Enhanced hairpin stability through loop design: the case of the protein G B1 domain hairpin. J Am Chem Soc 2004;126:7238–7243.
9. Espinosa JF, Munoz V, Gellman SH. Interplay between hydrophobic cluster and loop propensities in β-hairpin formation. J Mol Biol 2001;306:397–402.
10. Cochran AG, Skelton NJ, Starovasnik MA. Tryptophan zippers: stable, monomeric β-hairpins. Proc Natl Acad Sci USA 2001;98:5578–5583.
11. Pastor MT, Lopez del la Paz M, Lacroix E, Serrano L, Perez-Paya E. Combinatorial approaches: a new tool to search for highly structured β-hairpin peptides. Proc Natl Acad Sci USA 2002;99:614–619.
12. Ramírez-Alvarado M, Blanco F, Serrano L. Elongation of the BH8 β-hairpin peptide: electrostatic interactions in β-hairpin formation and stability. Protein Sci 2001;10:1381–1392.
13. Ciani B, Jourdan M, Searle MS. Stabilization of beta-hairpin peptides by salt bridges: role of preorganization in the energetic contribution of weak interactions. J Am Chem Soc 2003;125:9038–9047.
14. Galzitskaya OV, Higo J, Finkelstein AV. Alpha-helix and beta-hairpin folding from experiment, analytical theory and molecular dynamics simulations. Curr Protein Pept Sci 2002;3:191–200.
15. Kolinski A, Ilkowski B, Skolnick J. Dynamics and thermodynamics of beta-hairpin assembly: insights from various simulation techniques. Biophys J 1999;77:2942–2952.
16. Ma B, Nussinov R. Molecular dynamics simulations of a beta-hairpin fragment of protein G: balance between side-chain and backbone forces. J Mol Biol 2000;296:1091–1104.
17. Santiveri CM, Jimenez MA, Rico M, Van Gunsteren WF, Daura X. beta-hairpin folding and stability: molecular dynamics simulations of designed peptides in aqueous solution. J Pept Sci 2004;10:546–565.
18. Klimov DK, Thirumalai D. Mechanisms and kinetics of beta-hairpin formation. Proc Natl Acad Sci USA 2000;97:2544–2549.

19. Kobayashi N, Endo S, MuneKata E. Conformational study on the IgG binding domain of protein G. In: Yanaihara N, editor. Peptide Chem. Leiden, The Netherlands: ESCOM; 1993. p 278–280.
20. Blanco FJ, Rivas G, Serrano L. A short linear peptide that folds into a native stable β-hairpin in aqueous solution. Nature Struct Biol 1994;1:584–590.
21. Hutchinson EG, Sessions RB, Thornton JM, Woolfson DN. Determinants of strand register in antiparallel β-sheets of proteins. Protein Sci 1998;7:2287–2300.
22. Wouters MA, Curmi PMG. An analysis of side chain interactions and pair correlations within antiparallel β-sheets: the differences between backbone hydrogen-bonded and non-hydrogen-bonded residue pairs. Proteins 1995;22:119–131.
23. Gallagher T, Alexander P, Bryan P, Gilliland GL. Two crystal structures of the B1 immunoglobulin-binding domain of streptococcal protein G and comparison with NMR. Biochemistry 1994;33: 4721–4729.
24. Maynard AJ, Sharman GJ, Searle MS. Origin of β-hairpin stability in solution: structural and thermodynamic analysis of the folding of a model peptide supports hydrophobic stabilization in water. J Am Chem Soc 1998;120:1996–2007.
25. Hutchinson EG, Thornton JM. PROMOTIF: a program to identify and analyze structural motifs in proteins. Protein Sci 1996;5:212–220.
26. Wilmot CM, Thornton JM. Analysis and prediction of the different types of β-turn in proteins. J Mol Biol 1988;203:221–232.
27. Sibanda BL, Blundell TL, Thornton JM. Conformation of beta-hairpins in protein structures. J Mol Biol 1989;206:759–777.
28. Wilmot CM, Thornton JM. Beta-turns and their distortions: a proposed new nomenclature. Protein Eng 1990;3:479–493.
29. Penel S, Dobson PD, Mortishire-Smith RJ, Doig AJ. Length preferences and periodicity in β-strands. Antiparallel edge β-sheets are more likely to finish in non-hydrogen bonded rings. Protein Eng 2003;16:957–961.
30. Honda S, Kobayashi N, MuneKata E. Thermodynamics of a β-hairpin: evidence for cooperative formation of folding nucleus. J Mol Biol 2000;295:269–278.
31. Kobayashi N, Honda S, Yoshii H, MuneKata E. Role of side-chains in the cooperative β-hairpin folding of the short C-terminal fragment derived from streptococcal protein G. Biochemistry 2000;39:6564–6571.
32. Santiveri CM, Santoro J, Rico M, Jimenez MA. Thermodynamic analysis of β-hairpin-forming peptides from the thermal dependence of ^{1}H NMR chemical shifts. J Am Chem Soc 2002;124:14903–14909.
33. Tsai J, Levitt M. Evidence of turn and salt bridge contributions to beta-hairpin stability: MD simulations of C-terminal fragment from the B1 domain of protein G. Biophys Chem 2002;101–102, 187–201.
34. Pace CN, Vajdos F, Fee L, Grimsley GR, Gray T. How to measure and predict the molar absorption coefficient of a protein. Protein Sci 1995;4:2411–2423.
35. Delaglio F, Grzesiek S, Vuister G, Zhu G, Pfeifer J, Bax A. NMRPipe: a multidimensional spectral processing system based on UNIX Pipes. J Biomol NMR 1995;6:277–293.
36. Cavanagh J, Fairbrother WJ, Palmer AGI, Skelton NJ. Protein NMR Spectroscopy: principles and practice. San Diego: Academic Press; 1996. p 167–168.
37. Levitt M. Potential energy function and parameters for simulation of the molecular dynamics of proteins and nucleic acids in solution. Comp Phys Commun 1995;91:215–231.
38. Daggett V, Levitt M. A model of the molten globule state from molecular dynamics simulations. Proc Natl Acad Sci USA 1992;89: 5142–5146.
39. Grindley T, Lind JE. Pvt properties of water and mercury. J Chem Phys 1971;54:3983–3989.
40. Vedam R, Holton G. Specific volumes of water at high pressures obtained from ultrasonic-propagation measurements. J Acoust Soc Am 1968;43:108–116.
41. DeLano WL. The PyMOL molecular graphics system. San Carlos, CA: DeLano Scientific; 2002.
42. Kabsch W. Discussion of solution for best rotation to relate 2 sets of vectors. Acta Crystallogr A 1978;34:827–828.
43. Becker RA, Chambers JM, Wilks AR. The new S language. New York: Chapman & Hall; 1988.
44. Gerstein M, Tsai J, Levitt M. The volume of atoms on the protein surface: calculated from simulation, using Voronoi polyhedra. J Mol Biol 1995;249:955–966.
45. Munoz V, Thompson PA, Hofrichter J, Eaton WA. Folding dynamics and mechanism of beta-hairpin formation. Nature 1997;390: 196–199.
46. Syud FA, Espinosa JF, Gellman SH. NMR-based quantification of β-sheet populations in aqueous solution through use of reference peptides for the folded and unfolded states. J Am Chem Soc 1999;121:11577–11578.
47. Blanco F, Serrano L. Folding of protein G B1 domain studied by the conformational characterization of fragments comprising its secondary structure elements. Eur J Biochem 1995;230:634–649.
48. Buck M. Trifluoroethanol and colleagues: cosolvents come of age. Recent studies with peptides and proteins. Q Rev Biophys 1998;31: 297–355.
49. Wuthrich K. NMR of proteins and nucleic acids: John Wiley & Sons, Inc; 1986. 17 p.
50. Perczel A, Hollosi M. Turns. In: Fasman GD, editor. Circular dichroism and the conformational analysis of biomolecules. New York: Plenum Press; 1996. p 285–380.
51. Woody R, Dunker A. Aromatic and cystine side-chain circular dichroism in proteins. In: Fasman GD, editor. Circular dichroism and the conformational analysis of biomolecules. New York: Plenum Press; 1986. p 109–158.
52. Baldwin RL. How Hofmeister ion interactions affect protein stability. Biophys J 1996;71:2056–2063.
53. Bystroff C, Thorsson V, Baker D. HMMSTR: a hidden Markov model for local sequence-structure correlations in proteins. J Mol Biol 2000;301:173–190.
54. Karplus PA. Experimentally observed conformation-dependent geometry and hidden strain in proteins. Protein Sci 1996;5:1406–1420.
55. Searle M, Griffiths-Jones S, Skinner-Smith H. Energetics of weak interactions in a β-hairpin peptide: electrostatic and hydrophobic contributions to stability from lysine salt bridges. J Am Chem Soc 1999;121:11615–11620.
56. Kraulis PJ. MOLSCRIPT: a program to produce both detailed and schematic plots of protein structures. J Appl Crystallogr 1991;24: 946–950.